



Contents list available at CBIORE journal website








International Journal of Renewable Energy Development

Journal homepage: <https://ijred.cbiorc.id>



Research Article

Electrical and morphological variations with sintering temperature of electron transport layer in perovskite solar cell

Muhazri Abd Mutalib^a , Norasikin Ahmad Ludin^{a*} , Vincent Barrioz^b , Suhaila Sepeai^a ,
Mohd Sukor Su'ait^a , Muhammad Ubaidah Syafiq Mustaffa^a , Puvaneswaran Chelvanathan^a 

^a Solar Energy Research Institute (SERI), Universiti Kebangsaan Malaysia (UKM), 43600 Bangi, Selangor, Malaysia

^b Department of Mathematics, Physics and Electrical Engineering, Ellison Building, Northumbria University, Newcastle upon Tyne, NE1 8ST, United Kingdom

Abstract. The typical PSCs essentially made up of electron transporting material (compact and mesoporous), perovskite absorber layer and hole transporting material. The compact TiO₂ primary function is allow the movement of photogenerated electron to the device circuit from the active layer and to block the photogenerated holes from recombination at TCO substrate. Mesoporous TiO₂ mainly functions to receive the photogenerated charge from the perovskite absorber and enable thicker formation of perovskite absorber due to the voids in the TiO₂ mesoscopic framework. Many studies have implemented 500 °C as the standard in sintering the TiO₂ layer. However, the effects of sintering temperature of ETL TiO₂ have never been systematically described in terms of morphology and photoelectrochemical properties. In this manuscript, we have studied the morphological and photoelectrochemical properties of ETM TiO₂ thin film prepared at different sintering temperature. Spin coated TiO₂ layers were examined using X-ray Diffraction for crystal structure and phase identification, FESEM for morphological analysis, UV-Vis Spectroscopy for optical absorbance and transmittance of light and PEC test for LSV, EIS and TPC analyses. Surface roughness was not a major influencing factor of photocurrent density rather than the anatase phase of the TiO₂ thin film is more important. It was revealed that at 500 °C, the TiO₂ thin film possess the highest photocurrent density with good stability and lowest charge transfer and series resistance. Higher sintering temperature of 550 °C, would introduce lattice defects in the TiO₂ thin film which will reduce photocurrent density and increase resistance. This work offers a systematic evaluation of the ETL in terms of morphological and photoelectrochemical properties, which can be applied when selecting suitable material for ETL in perovskite solar devices.

Keywords: perovskite solar cells; electron transport layer; TiO₂; sintering temperature; charge transfer resistance



© The author(s). Published by CBIORE. This is an open access article under the CC BY-SA license (<http://creativecommons.org/licenses/by-sa/4.0/>).

Received: 7th Nov 2024; Revised: 17th April 2025; Accepted: 28th May 2025; Available online: 15th June 2025

1. Introduction

Perovskite solar cells (PSCs) have been considered one of the most promising solar cell technologies because of its high photoconversion efficiency, which rivals that of high strain-fabricated crystalline silicon solar cells (Abd Mutalib, Aziz, *et al.*, 2018). Silicon-based solar cells have traditionally dominated the market, but metal halide PSCs have quickly emerged as a highly promising alternative (Han *et al.*, 2025). Though still relatively new, PSCs are advancing at an exceptional pace, propelled by intensive global research efforts that leverage their distinctive advantages. These promising cells boast lower production costs, simpler fabrication methods, and superior mechanical flexibility compared to conventional silicon-based technologies.

Despite the presence of lead and the moisture susceptibility of the perovskite absorber layer (Abd Mutalib, Ahmad Ludin, *et al.*, 2018), the power conversion efficiency of PSCs has been on a steady ascension from 9% to 24.2% ("NREL Best Research-Cell Efficiencies," n.d.). Typical PSCs are made of electron transport layer (ETL; compact and mesoporous), perovskite absorber layer and hole transport layer (HTL). Nevertheless, in planar PSC design, where mesoporous ETL is omitted, is also sometimes applied allowing low temperature processing of the

PSC (Abd Mutalib, Ahmad Ludin, *et al.*, 2018). Past studies have outlined the optimum properties of primary materials for high-performance ETL. These properties include good electron mobility with low photocurrent resistance, wide band gap for high light transmission and compatible energy level with other PCS component layers (Lu, Ma, Gu, Tian, & Li, 2015). In addition, high light transmission can be achieved by the application of ETL material with low reflection to prevent light scattering. Compact TiO₂ (c-TiO₂) allows the movement of photogenerated electron from the active layer to the device circuit and blocks the recombination of photogenerated holes at the transparent conductive oxide (TCO) substrate (Wu *et al.*, 2015). The ETL must be continuous, uniform and thin to avoid the charge recombination between the perovskite layer and TCO substrate and prevent current leakage (Lee *et al.*, 2013). Thus, c-TiO₂ is imperative to produce highly efficient PSCs.

Later, new PSC structures have emerged. Such new PSCs include planar PSC, in which the mesoporous TiO₂ (m-TiO₂) layer is omitted from the structure (Liu, Johnston, & Snaith, 2013). The importance of m-TiO₂ was later revealed, that is, it receives the photogenerated charge from the perovskite absorber and enables the formation of thicker perovskite absorber because of the voids in the TiO₂ mesoscopic

* Corresponding author
Email: sheekeen@ukm.edu.my (N.A. Ludin)

framework (Mohamad Firdaus Mohamad Noh et al., 2018). The mesoporous structure provides a high surface area, which increases the charge transfer rate between the perovskite material and ETL (Meyer, 2010). Moreover, hysteresis effect mitigation and higher performance stability were achieved in PCS devices with m-TiO₂ compared with planar PCs.

Different methods of ETL deposition have been widely discussed and compared to date. ETL TiO₂ have been fabricated using various methods, including spin coating (Abd Mutalib et al., 2022; Im, Jang, Pellet, Grätzel, & Park, 2014), spray pyrolysis (Saliba et al., 2016), screen printing (Mahmood, Swain, & Amassian, 2015), sputtering (Chen, Cheng, Dai, & Song, 2015), atomic layer deposition and electrochemical deposition (Kavan, Tétreault, Moehl, & Grätzel, 2014). Most research have adopted the spin coating method probably because of its cost effectiveness, simple process and ease of use. The sintering temperature applied in spin coating is usually ~500 °C, which usually aimed at producing anatase TiO₂ (Green, Ho-Baillie, Snaith, & Martin A. Green, 2014). However, the effects of the sintering temperature of ETL TiO₂ have never been systematically described in terms of morphological and photoelectrochemical (PEC) properties.

In the effort to avoid high fabrication cost due to high energy requirement from high temperature (<450 °C), some have researched low energy requirement fabrication method (Im and Olasoji, 2024). Nevertheless, the resulting PCE from low temperature devices still cannot match the convention temperature treatment methods (Yoo et al., 2024). However, recent advancements in low-temperature deposition techniques have enabled the fabrication of perovskite solar devices on flexible substrates, marking a significant step toward lightweight, portable, and versatile photovoltaic technologies. These innovative methods, which typically operate below 150 °C, are compatible with polymer-based substrates that would otherwise degrade under conventional high-temperature processing. This breakthrough has opened new avenues for integrating perovskite solar cells into wearable electronics, roll-to-roll manufacturing, and building-integrated photovoltaics. Nevertheless, despite the promising potential, devices fabricated on flexible substrates generally exhibit lower performance metrics (reduced power conversion efficiency and operational stability), when compared to their counterparts built on rigid, thermally robust substrates like glass. This performance gap is often attributed to challenges such as poor film uniformity, suboptimal crystal quality, and increased defect densities that arise during low-temperature processing. As such, ongoing research is focused on optimizing deposition parameters and material formulations to enhance the efficiency and reliability of flexible perovskite solar devices.

In this manuscript, we studied the morphological and PEC properties of ETL TiO₂ thin film prepared at different sintering temperatures, namely, 450, 500 and 550 °C. The morphology and PEC properties of the spin-coated ETL TiO₂ were studied thoroughly. Spin coating method was chosen because of its simplicity, cost and ease of use. The results showed that the TiO₂ thin film sintered at 500 °C possessed the highest photocurrent density, good stability and lowest charge transfer and series resistance.

2. Material and Method

2.1 TiO₂ layer preparation

TiO₂ BL-1 blocking layer, 18NR-T Transparent Titania Paste and fluorine-doped tin oxide (FTO)-coated glass were

purchased from Greatcell Solar Materials (greatcellsolarmaterials.com). The FTO-coated glass substrates were etched to draw out the desired electrode pattern using zinc powder and HCl (3 M). The glass substrates were then washed consecutively with soap (2% Hellmanex in water), acetone and isopropanol to remove the organic residue on their surface. The chemicals were obtained from Sigma Aldrich and used as received. Firstly, approximately 100 nm c-TiO₂ layer was spin-coated at the surface of the active layer using BL-1 mixed with ethanol as the precursor and then heated to 150 °C. The m-TiO₂ layer (~400 nm) was then spin-coated using 18 NR-T paste and then sintered at different temperatures for 60 min. Both c-TiO₂ and m-TiO₂ were spin-coated at 3000 r/min for 60 s. The TiO₂ thin films sintered at different temperatures (450, 500 and 550 °C) are herein denoted as according to their sintering temperature.

2.2 Characterization

The characterization part in this manuscript is consisted of physical, optical and PEC characterizations. Physical characterization consists of X-ray diffraction (XRD), Atomic Force Microscopy (AFM) and Field-emission scanning electron microscope (FESEM). Optical characterization consists of UV-visible spectrophotometer. Finally, the PEC characterization consists of linear sweep voltammetry (LSV) and electrochemical impedance spectroscopy (EIS).

2.3 Physical Characterization

The crystal structure of the TiO₂ thin films was determined via XRD using a Bruker D8 Advance operated at 2θ angle in the range of 20°–70°. The crystal structure of the TiO₂ has to be identified because one of the polymorphs has the best properties for electron transport layer application. The data findings were then processed using Diffrac Suite EVA software evaluation to obtain crystallinity percentage of the samples. The thickness of the films was measured using a profilometer (Dektak XT, Bruker). The surface roughness of the TiO₂ thin films is measured using Nanosurf Easyscan 2 AFM by Park Systems. A variation in surface roughness may serve as an indicator of alterations in the crystal structure of the sample. Such changes often reflect underlying modifications in the material's microstructure, which can arise from differences in processing conditions, phase transitions, or the incorporation of dopants or defects. The surface morphology of the TiO₂ films were analysed using a FESEM using a SUPRA VP55.

2.4 Optical Characterization

Specular transmittance measurements were carried out at room temperature, in the wavelength range of 300 – 1000 nm, using a UV-visible spectrophotometer (Lambda 35, PerkinElmer) to investigate the optical properties of the samples. The optical properties will allow to inspect over the absorption and transmittance range the samples with different sintering temperature and also detects the change in band gap (eV). The band gap values also allow the detection crystal structure of TiO₂ as compared to previous study.

2.5 Photoelectrochemical Characterization

The PEC properties of the TiO₂ films were determined via LSV and EIS using an electrochemical workstation (Metrohm Autolab) in the dark and under visible light illumination (simulated AM 1.5 at a calibrated intensity 100 mW/cm²) at room temperature and atmospheric pressure. The TiO₂ thin

film-coated FTO substrate with an active area of 1.0 cm² was dipped in 40 ml of aqueous 0.5 M Na₂SO₄ solution and connected to the workstation as the working electrode. Pt electrode was used as the counter electrode, and Ag/AgCl electrode was used as the reference electrode (RE). For LSV measurement, a scanning rate of 10 mV/s, in the potential range of -0.4 – 1.4 V with respect to RE, was applied. EIS measurement was carried out at the frequency range of 105 – 0.1 Hz and the bias voltage of 0.0 V with respect to RE.

3. Results and Discussion

3.1 X-ray Diffraction

The XRD patterns of all the TiO₂ thin films were determined to examine the changes in crystallinity and crystallite size, with respect to temperature variation between 450 °C to 550 °C. Higher crystallinity would allow higher charge transfer along the thin film with lower probability to encounter crystal defects. It was proven that TiO₂ with anatase crystal structure is a preferred TiO₂ forms rather than rutile crystal structure due to the epitaxial growth of TiO₂ grains producing higher electron mobility in anatase form (Luttrell *et al.*, 2015). While rutile TiO₂ is thermodynamically stable at high temperatures, anatase TiO₂ is typically preferred for photo-related applications due to its higher surface area, better electron mobility, and longer electron lifetime, which contribute to enhanced photocatalytic and photovoltaic performance (Luttrell *et al.*, 2014). Additionally, when using spin coating technique to deposit the perovskite active layer, the perovskite precursor solution can be easily deposited onto a highly crystalline ETL (Ye *et al.*, 2017). As Figure 1 suggests, all samples have no remarkable changes in XRD pattern and exhibited the typical anatase crystal structure of TiO₂ diffraction peaks at 25.7° (101), 38.2° (004), 48.4° (200) and 55.0° (211) (JCPDS card no. 21-1272).

Additional XRD peaks attributed to the FTO underlayer is depicted in Fig. 1.

The Scherrer equation was applied to the main diffraction peaks in the diffraction pattern and averaged to estimate the crystalline size of the deposited TiO₂ thin film.

$$D = \frac{K\lambda}{\beta \cos \theta} \quad (1)$$

where D is the average crystallite size in angstroms (Å), K is the shape factor taken as 0.9, λ is the wavelength of X-ray radiation (1.5406 Å), β is the FWHM after appropriate base line correction, and θ is the diffraction angle. The prepared samples were differentiated according to degree of crystallinity and crystallite size. Table 1 shows the crystallite size, crystallinity percentage, layer thickness and surface roughness of all samples. As described in the table, the crystallite size and crystallinity percentage tend to increase as the temperature increases. As revealed in previous study, the increase in crystallite size is an indication of structural change from anatase to rutile, suggesting the crystallite growth according to the Ostwald-ripening mechanism (Chao, Petrovsky, & Dogan, 2010). Additionally, the atomic force microscopy and profilometer results revealed an increase in the surface roughness and layer thickness of TiO₂-550.

Surface roughness plays an important role towards the performance of photoanode thin film, where previous study have elaborated the increase in surface roughness would lead to higher number of active photocatalytic sites on the surface (Noh *et al.* 2018). The surface roughness of a thin film is closely associated with the availability of photocatalytic sites, which influences photocurrent performance. Previous studies have explained that the increased surface roughness is a result of the unique grain behavior of rutile TiO₂. The rutile phase tends to exhibit more irregular grain growth, leading to larger, more pronounced surface features and grain boundaries, which

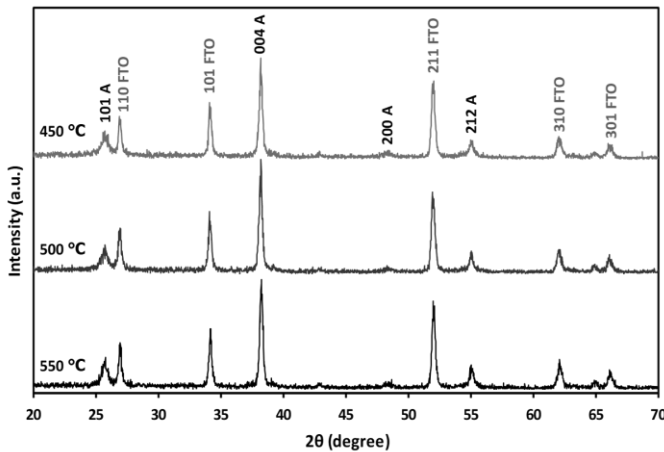


Fig. 1 XRD patterns of TiO₂ thin films sintered at different temperatures.

Table 1
Crystallite size and crystallinity percentage of the prepared samples

Temperature, °C	Crystallite size, nm	Crystallinity percentage, %	Layer thickness, nm	Surface roughness, nm
450	27.38	85.7	538.4	4.9
500	30.05	86.4	576.3	5.0
550	31.79	86.7	620.1	17.3

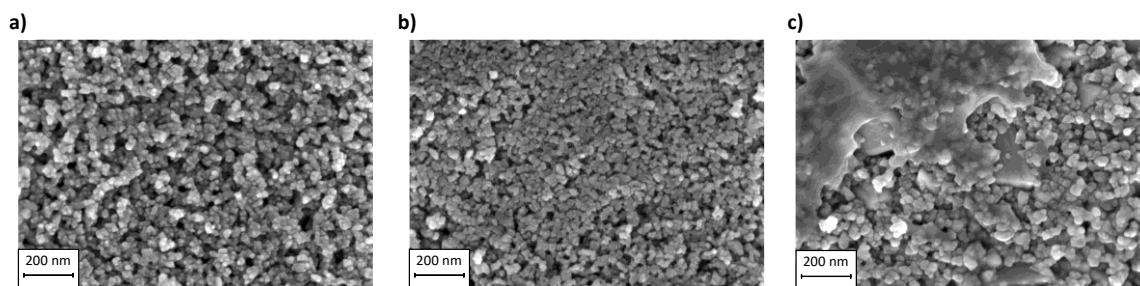


Fig. 2 FESEM images of the surface of (a) TiO₂-450, (b) TiO₂-500 and (c) TiO₂-550.

contribute to the enhanced roughness (Luttrell *et al.*, 2014). The grains exhibit a mildly rectangular morphology, with two distinct types oriented perpendicular to each other at 90°. The increase in surface roughness at different sintering temperatures was further analysed with the photocurrent performance of TiO₂ thin film.

3.2 Surface Morphology

The morphological properties of the spin-coated TiO₂ thin films sintered at different temperatures were examined by FESEM. Figure 2 shows the top view of the prepared TiO₂ films. The surfaces of the TiO₂ thin films have good coverage over the substrate surface without the presence of cracks and with a relatively porous structure. The compactness of the layer increased (i.e. decrease in porosity) as the sintering temperature increased. A similar effect was reported in a previous study, in which a higher degree of film compactness was successfully achieved through the use of magnetron sputtering. This technique facilitated the formation of a denser and more uniform layer, thereby enhancing the material's structural and functional properties, which are critical for improving device performance and stability (Zhang *et al.*, 2016). Most importantly, in Figure 2(c), the surface of TiO₂ thin film starts to agglomerate while exposing the underlayer features (c-TiO₂) and diminishing the porous structure of the thin film. The TiO₂ layer maintains its anatase structural stability at 450–500 °C and partly transforms to rutile phase at 550 °C (Gao *et al.*, 2008). Thus, Figure 2(c) shows some indication of phase change (agglomeration) at the surface of the TiO₂ thin film. High temperature endorses agglomeration and pore collapse and thus diminishes the active surface areas of the thin film (Gomes *et al.*, 2019). Likewise, later, the UV-Vis results have indicated

the phase change of anatase to rutile by the change in the band gap of the thin film.

3.3 Optical Properties

One of the key requirements for achieving a high-performance electron transport layer (ETL) in perovskite solar cells is the use of a material that possesses a wide band gap and exhibits high optical transparency. This characteristic is essential to ensure minimal parasitic absorption within the ETL itself, thereby allowing maximum transmission of incident light to the underlying perovskite absorber layer, which is critical for efficient photon harvesting and overall device performance (Mohamad Firdaus Mohamad Noh *et al.*, 2018b). The optical properties of the prepared TiO₂ thin film sample were examined using UV-Vis spectrometer and are shown in Figure 3. All absorption spectra show typical TiO₂ absorption, increasing as it approaches the UV region (Yang *et al.*, 2017). The light absorption ability of the thin films increased with the sintering temperature. This phenomenon was portrayed in Figure 3(a), where higher light absorption would translate to less photons reaching to the light absorbing layer (perovskite). The inset in Figure 3(a) shows the Tauc's plot, which was used to estimate the band gap energy of the TiO₂ thin films. The band gap displayed a descending pattern as the sintering temperature increases. The band gap values of TiO₂-450, TiO₂-500 and TiO₂-550 °C were 3.25, 3.18 and 3.0 eV, respectively. The band gap energy values were relatively similar with previous study where the band gap values are correlated with the phase of TiO₂ (anatase at 3.27 eV or rutile at 2.95 eV) (Yang *et al.*, 2017). Notably, the band gap values confirmed the phase change of the TiO₂ thin film from anatase to rutile with the increase in sintering temperature from 500 °C to 550 °C.

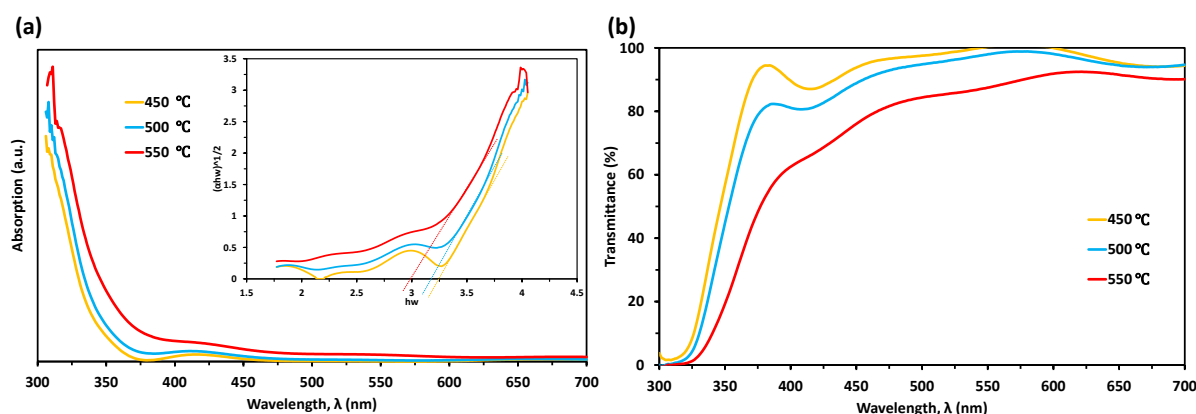


Fig. 3 (a) Absorption and (b) transmission spectra of the TiO₂ thin films sintered at different temperatures.

The light transmission spectra of the prepared TiO₂ thin films are shown in Figure 3(b). All the transmittance spectra showed typical TiO₂ thin film response with low transparency at the UV range of the wavelength, as expected due to the nature of the material with such bandgap (Chibani, Challali, Touam, Chelouche, & Djouadi, 2019). The figure shows a reduction in light transmission as the TiO₂ sintering temperature increased. The reduction in light transmission may be related to the higher absorbance and layer thickness in higher sintering temperature samples. Additionally, high surface roughness at 550 °C could also contribute to lower transparency as similarly reported in a previous study (Soh-Yusoff *et al.*, 2019). Surface irregularities lead to the scattering of incident light, thereby reducing the intensity of the transmitted light. This phenomenon has been previously documented and analyzed in earlier studies, which highlight the significant impact of surface morphology on light transmission efficiency (Li *et al.*, 2004).

3.4 Photoelectrochemical Properties

In the photoelectrochemical properties evaluation, the sintering temperatures of TiO₂ thin film is set with 50 °C interval between the samples (450 °C, 500 °C and 550 °C). PEC performance test was set up on a three-electrode configuration to evaluate the charge transport properties of the deposited TiO₂ thin films prepared at different sintering temperatures, and the results are shown in Figure 4. The low light absorption of TiO₂ thin film decreased the photoinduced charge carrier generation in the thin film. Based on the figure, the highest photocurrent density at 1.0 V was observed in TiO₂-500 with 104.67 µA/cm² as shown in Table 2. This result indicates that while surface roughness can influence device performance, it is not the sole contributing factor responsible for the enhancement of photocurrent density. Other parameters, such as film crystallinity, interface quality, charge transport properties, and the presence of defects or trap states, may also play significant roles in determining the overall photoresponse of the device.

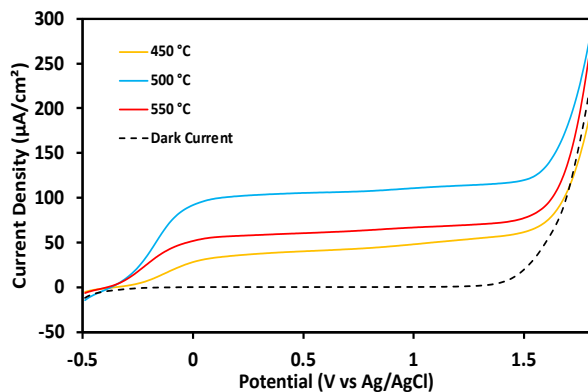


Fig. 4 Photocurrent density versus potential curves of the sintered TiO₂ thin films.

Table 2
Photocurrent density of TiO₂ thin films sintered at different temperatures

TiO ₂ sintering temperature, °C	Photocurrent density µA/cm ²
450	50.41
500	104.67
550	55.58

The difference in the photocurrent densities between TiO₂-450 and TiO₂-500 is closely related to the increase in crystallinity percentage, the reduction in crystallite size and the increase in layer compactness. However, the decrease in the photocurrent density of TiO₂-550 may be related to the formation of aggregates (crystal defects) in the TiO₂ thin film, which precedes the phase transformation of TiO₂. These aggregates, albeit produced high surface roughness, can introduce lattice defects, which can become charge recombination sites in the thin film and reduce the photocurrent generation of the thin film (Wu *et al.*, 2014).

EIS measurement was performed to determine the effects of temperature on the charge transfer characteristic of the thin films. The Nyquist plot of all TiO₂ thin films measured in the presence of light at 0 V bias voltage is shown in Figure 5. In general, the Nyquist plot displays at least one semicircle, which corresponds to an [R(RC)] component. Charge transfer resistance (RCT) is represented by the diameter of the semicircle arc. Thus, a larger semicircle diameter means an increase in RCT, which is inversely proportional to the photocurrent. Based on Figure 5 and Table 3, TiO₂ thin film sintered at 500 °C had the lowest RCT, and highest RCT at 550 °C. This finding corresponds with the LSV results. The increase in the RCT at temperature 550 °C and above may be related to the phase change at high sintering temperature (~550°C). Additionally, the increase in RCT and series resistance (RS) may be associated with the increase in layer thickness (refer Table 1). This increase in resistance would lead to the low current density and fill factor of perovskite solar device (Noh *et al.*, 2018). The TiO₂-500 thin film had the lowest RCT may be due to the anatase phase of the TiO₂ thin film. A previous study reported similar findings that rutile-based TiO₂ thin film has lower electron transport property compared with anatase-based thin film (Yang *et al.*, 2017). The combination of a lower effective electron mass and an extended electron lifetime plays a crucial role in suppressing recombination processes within anatase thin films. The reduced effective mass facilitates more efficient charge carrier mobility, allowing electrons to traverse the material with less resistance. Simultaneously, the longer electron lifetime provides an extended window during which charge carriers can be collected before recombination occurs. Together, these factors significantly contribute to the inherently slower recombination rate observed in anatase-phase TiO₂ thin films, thereby enhancing their charge transport properties and overall performance in optoelectronic applications. Additionally, the lowest Rs values can also be found at sintering

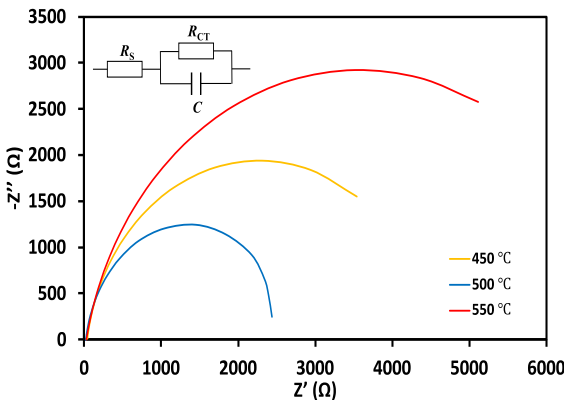


Fig. 5 Nyquist plot of the EIS responses of the TiO₂ thin films under light illumination.

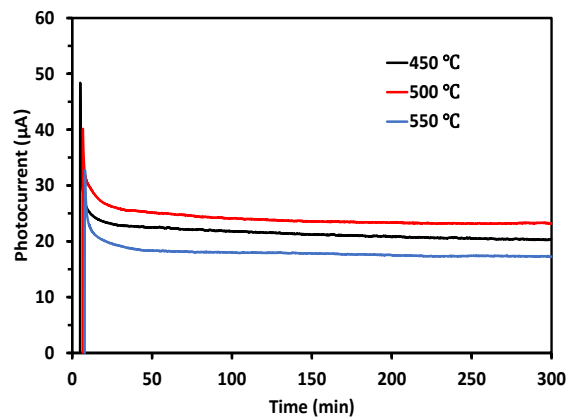


Fig. 6 Transient photocurrent graph TiO₂ thin films at different sintering temperatures measured at 1.0 V versus Ag/AgCl with illumination.

Table 3
Charge transfer resistance and series resistance of TiO₂ thin films prepared at different sintering temperature

Temperature, °C	R_{CT} , k Ω	R_s , Ω
450	5.530	32.9
475	2.857	25.0
500	2.655	20.6
525	2.990	21.9
550	7.086	28.9
575	8.084	28.7

temperature of 500 °C. Low R_s value would allow minimal hysteresis in the perovskite solar device (Upama *et al.*, 2017).

Previous studies have used the TPC signal to reveal the charge extraction dynamics and have demonstrated that the TPV signal is a good measure of the charge carrier density in the device, such that the transient decay corresponds well with the recombination rate of the photogenerated charge. Transient photocurrent measurement has been extensively used by previous literatures to study the charge extraction dynamics of the thin film, in such manner that the recombination rate of the photogenerated charge can be represented by the transient decay (Wood *et al.*, 2017). The transient photocurrent measurement of the spin-coated TiO₂ thin films prepared at different sintering temperatures was determined by measuring the photocurrent time dependence under light illumination. In Figure 6, TiO₂-500 displayed the highest photocurrent density, followed by TiO₂-450 and TiO₂-550. Additionally, ΔQ , total charge extracted, can be represented as the area under the curve in Figure 6 (Wood *et al.*, 2017). Thus, highest ΔQ is 500°C at 7.07 μC , followed by 450°C the 550 °C, with 6.35 μC and 5.23 μC , respectively. The trend in ΔQ results is coincidentally similar with the LSV and EIS results. All the TiO₂ samples displayed a rather stable performance under 300 min of illumination.

4. Conclusion

In summary, TiO₂ thin films as ETL were fabricated at different sintering temperatures. The thin films displayed typical TiO₂

response in XRD where crystal structure of anatase was observed for samples sintered at 450 °C and 500 °C. The observed increase in both crystallite size and surface roughness at a sintering temperature of 550 °C suggests a significant microstructural transformation indicative of a phase transition from the anatase to the rutile crystal structure in TiO₂. Such changes are critical, as they influence the optical, electrical, and catalytic properties of the TiO₂ film, making them highly relevant in tailoring material performance for specific applications. TiO₂-500 showed the highest photocurrent density and the lowest charge transfer and series resistance. Furthermore, the TiO₂ thin films were stable for 5 h of testing. Surface roughness was not a major influencing factor of photocurrent density rather than the anatase phase of the TiO₂ thin film is more important. The higher sintering temperature of more than 550 °C introduced phase change to rutile in the TiO₂ thin film, which reduced photocurrent density and increased resistance. The thin film surface played an important role for the presence of photocatalytic sites; nevertheless, the internal lattice of the thin film will determine the photocurrent density and resistance of the thin film, which are crucial for high-efficiency perovskite solar devices. This work offers a systematic evaluation of the ETL in terms of morphological and photoelectrochemical properties, which can be applied when selecting suitable material for ETL in perovskite solar devices.

Acknowledgments

The authors acknowledge the financial support by the Universiti Kebangsaan Malaysia (UKM) under the Dana Impak Perdana 2.0 (DIP-2024-003), Modal Insan (MI-2017-007) and Geran Universiti Penyelidikan (GUP-2024-108). The authors would also like to acknowledge technical and management support from the Centre for Research and Instrumentation (CRIM), UKM. The first author also would like to acknowledge UKM for PhD scholarship under the Skim Zamalah Yayasan Canselor 2016.

Author Contributions: M.A.M.: Conceptualization, methodology, formal analysis, writing—original draft, N.A.L.; supervision, resources, project administration, V.B., S.S., M.S.S., M.A.M.T., M.A.I.; writing—review and editing, project administration, validation, All authors have read and agreed to the published version of the manuscript.

Funding: This research was funded by Dana Impak Perdana 2.0 (DIP-2024-003), Modal Insan (MI-2017-007) and Geran Universiti Penyelidikan (GUP-2024-108).

Conflicts of Interest: The authors declare no conflict of interest.

References

Abd Mutalib, M., Ahmad Ludin, N., Nik Ruzalman, N. A. A., Barrioz, V., Sepeai, S., Mat Teridi, M. A., Su'ait, M. S., Ibrahim, M. A. & Sopian, K. (2018). Progress towards highly stable and lead-free perovskite solar cells. *Materials for Renewable and Sustainable Energy*, 7(2), 7. <https://doi.org/10.1007/s40243-018-0113-0>

Abd Mutalib, M., Ahmad Ludin, N., Su'ait, M. S., Davies, M., Sepeai, S., Mat Teridi, M. A., Noh, M. F. M. & Ibrahim, M. A. (2022). Performance-Enhancing Sulfur-Doped TiO₂ Photoanodes for Perovskite Solar Cells. *Applied Sciences*, 12(1), 429. <https://doi.org/10.3390/app12010429>

Abd Mutalib, M., Aziz, F., Fauzi, A., Norharyati, W., Salleh, W., Yusof, N., Jaafar, J., Soga, T., Sahdan, M. Z. & Ludin, N. A. (2018). Towards high performance perovskite solar cells : A review of

- morphological control and HTM development. *Applied Materials Today*, 13, 69–82. <https://doi.org/10.1016/j.apmt.2018.08.006>
- Amore Bonapasta, A., Filippone, F., Mattioli, G., & Alippi, P. (2009). Oxygen vacancies and OH species in rutile and anatase TiO₂ polymorphs. *Catalysis Today*, 144(1–2), 177–182. <https://doi.org/10.1016/j.cattod.2009.01.047>
- Chao, S., Petrovsky, V., & Dogan, F. (2010). Effects of sintering temperature on the microstructure and dielectric properties of titanium dioxide ceramics. *Journal of Materials Science*, 45(24), 6685–6693. <https://doi.org/10.1007/s10853-010-4761-4>
- Chen, C., Cheng, Y., Dai, Q., & Song, H. (2015). Radio Frequency Magnetron Sputtering Deposition of TiO₂ Thin Films and Their Perovskite Solar Cell Applications. *Scientific Reports*, 5. <https://doi.org/10.1038/srep17684>
- Chibani, O., Challali, F., Touam, T., Chelouche, A., & Djouadi, D. (2019). Optical waveguiding characteristics of TiO₂ sol–gel thin films for photonic devices: effects of thermal annealing. *Optical Engineering*, 58(04), 1. <https://doi.org/10.1117/1.oe.58.4.047101>
- Di Giacomo, F., Zardetto, V., D'Epifanio, A., Pescetelli, S., Matteocci, F., Razza, S., Di Carlo, A., Licoccia, S., Kessels, W. M. M., Creatore, M., & Brown, T. M. (2015). Flexible Perovskite Photovoltaic Modules and Solar Cells Based on Atomic Layer Deposited Compact Layers and UV-Irradiated TiO₂ Scaffolds on Plastic Substrates. *Advanced Energy Materials*, 5(8), 1401808–1401817. <https://doi.org/10.1002/aenm.201401808>
- Gao, S. A., Xian, A. P., Cao, L. H., Xie, R. C., & Shang, J. K. (2008). Influence of calcining temperature on photoresponse of TiO₂ film under nitrogen and oxygen in room temperature. *Sensors and Actuators, B: Chemical*, 134(2), 718–726. <https://doi.org/10.1016/j.snb.2008.06.017>
- Gomes, J., Lincho, J., Domingues, E., Quinta-Ferreira, R., & Martins, R. (2019). N–TiO₂ Photocatalysts: A Review of Their Characteristics and Capacity for Emerging Contaminants Removal. *Water*, 11(2), 373. <https://doi.org/10.3390/w11020373>
- Green, M. A., Ho-Baillie, A., Snaith, H. J., & Martin A. Green, A. H.-B. and H. J. S. (2014). The emergence of perovskite solar cells. *Nat Photon*, 8(7), 506–514. <https://doi.org/10.1038/nphoton.2014.134>
- Han, J., Park, K., Tan, S., Vaynzof, Y., Xue, J., Diao, E.W.-G., Bawendi, M.G., Lee, J.-W., Jeon, I., 2025. Perovskite solar cells. *Nature Reviews Methods Primers* 5, 3. <https://doi.org/10.1038/s43586-024-00373-9>
- Im, J. H., Jang, I. H., Pellet, N., Grätzel, M., & Park, N. G. (2014). Growth of CH₃NH₃PbI₃ cuboids with controlled size for high-efficiency perovskite solar cells. *Nature Nanotechnology*, 9(11), 927–932. <https://doi.org/10.1038/nnano.2014.181>
- Im, S.H., Olasoji, A.J., 2024. Perspective Chapter: TiO₂ Electron Transporting Layers for Perovskite Solar Cells, in: Montalvo Romero, C., Aguilar, C.A., Moctezuma, E. (Eds.), Titanium Dioxide - Uses, Applications, and Advances. IntechOpen, Rijeka. <https://doi.org/10.5772/intechopen.1007266>
- Kavan, L., T  treault, N., Moehl, T., & Gr  tzel, M. (2014). Electrochemical characterization of TiO₂ blocking layers for dye-sensitized solar cells. *Journal of Physical Chemistry C*, 118(30), 16408–16418. <https://doi.org/10.1021/jp4103614>
- Heo, J. H., Im, S. H., Noh, J. H., Mandal, T. N., Lim, C.-S., Chang, J. A., Lee, Y. H., Kim, H.-j., Sarkar, A., Nazeeruddin, M. K., Gratzel, M., & Seok, S. Il. (2013). Efficient inorganic–organic hybrid heterojunction solar cells containing perovskite compound and polymeric hole conductors. *Nature Photonics*, 7(6), 486–491. <https://doi.org/10.1038/nphoton.2013.80>
- Li, C., Kattawar, G.W., Yang, P., 2004. Effects of surface roughness on light scattering by small particles. *J Quant Spectrosc Radiat Transf* 89, 123–131. <https://doi.org/10.1016/j.jqsrt.2004.05.016>
- Liu, M., Johnston, M. B., & Snaith, H. J. (2013). Efficient planar heterojunction perovskite solar cells by vapour deposition. *Nature*, 501(7467), 395–398. <https://doi.org/10.1038/nature12509>
- Lu, H., Ma, Y., Gu, B., Tian, W., & Li, L. (2015). Identifying the optimum thickness of electron transport layers for highly efficient perovskite planar solar cells. *Journal of Materials Chemistry A*, 3(32), 16445–16452. <https://doi.org/10.1039/c5ta03686k>
- Luttrell, T., Halpegamage, S., Tao, J., Kramer, A., Sutter, E., & Batzill, M. (2015). Why is anatase a better photocatalyst than rutile? - Model studies on epitaxial TiO₂ films. *Scientific Reports*, 4, 282. <https://doi.org/10.1038/srep04043>
- Mahmood, K., Swain, B. S., & Amassian, A. (2015). 16.1% Efficient Hysteresis-Free Mesoporous Perovskite Solar Cells Based on Synergistically Improved ZnO Nanorod Arrays. *Advanced Energy Materials*, 5(17), 1500568. <https://doi.org/10.1002/aenm.201500568>
- Meyer, G. J. (2010). The 2010 Millennium Technology Grand Prize: Dye-Sensitized Solar Cells. *ACS Nano*, 4(8), 4337–4343. <https://doi.org/10.1021/nn101591h>
- Mohamad Noh, Mohamad F., Soh, M. F., Riza, M. A., Safaei, J., Mohd Nasir, S. N. F., Mohamad Sopian, N. W., Yap, C. C., Ibrahim, M. A., Ludin, N. A. & Mat Teridi, M. A. (2018). Effect of Film Thickness on Photoelectrochemical Performance of SnO₂ Prepared via AACVD. *Physica Status Solidi (B) Basic Research*, 255(6). <https://doi.org/10.1002/pssb.201700570>
- Mohamad Noh, Mohamad Firdaus, Teh, C. H., Daik, R., Lim, E. L., Yap, C. C., Ibrahim, M. A., Ludin, N. A., Yusoff, A. R. M., Jang, J. & Mat Teridi, M. A. (2018). The architecture of the electron transport layer for a perovskite solar cell. *Journal of Materials Chemistry C*, 6(4), 682–712. <https://doi.org/10.1039/c7tc04649a>
- NREL Best Research-Cell Efficiencies. (n.d.). Retrieved November 9, 2016, from <https://www.nrel.gov/pv/cell-efficiency.html>
- Saliba, M., Matsui, T., Seo, J.-Y., Domanski, K., Correa-Baena, J.-P., Nazeeruddin, M. K., Zakeeruddin, S. M., Tress, W., Abate, A., Hagfeldt, A. & Gr  tzel, M. (2016). Cesium-containing Triple Cation Perovskite Solar Cells: Improved Stability, Reproducibility and High Efficiency. *Energy Environ. Sci.*, 9(6), 1989–1997. <https://doi.org/10.1039/C5EE03874J>
- Soh-Yusoff, M. F., Noh, M. F. M., Teh, C. H., Ludin, N. A., Ibrahim, M. A., Teridi, M. A. M., & Yusoff, A. R. M. (2019). Kesan Ketebalan Filem Terhadap Fotoelektrokimia Titania Dioksida (TiO₂) Yang Disediakan Melalui Kaedah Pemendapan Bantuan Aerosol Wap Kimia (AACVD). *Jurnal Kejuruteraan*, 31(1), 85–92. [https://doi.org/10.17576/jjukm-2019-31\(1\)-10](https://doi.org/10.17576/jjukm-2019-31(1)-10)
- Upama, M. B., Elumalai, N. K., Mahmud, M. A., Wang, D., Haque, F., Gon  ales, V. R., Gooding, J. J., Wright, M., Xu, C. & Uddin, A. (2017). Role of fullerene electron transport layer on the morphology and optoelectronic properties of perovskite solar cells. *Organic Electronics: Physics, Materials, Applications*, 50, 279–289. <https://doi.org/10.1016/j.orgel.2017.08.001>
- Wood, S., O'Connor, D., Jones, C. W., Claverley, J. D., Blakesley, J. C., Giusca, C., & Castro, F. A. (2017). Transient photocurrent and photovoltage mapping for characterisation of defects in organic photovoltaics. *Solar Energy Materials and Solar Cells*, 161, 89–95. <https://doi.org/10.1016/j.solmat.2016.11.029>
- Wu, R., Yang, B., Xiong, J., Cao, C., Huang, Y., Wu, F., Sun, J., Zhou, C., Huang, H. & Yang, J. (2015). Dependence of device performance on the thickness of compact TiO₂ layer in perovskite/TiO₂ planar heterojunction solar cells. *Journal of Renewable and Sustainable Energy*, 7(4), 043105. <https://doi.org/10.1063/1.4926578>
- Wu, Y., Yang, X., Chen, H., Zhang, K., Qin, C., Liu, J., Peng, W., Islam, A., Bi, E. & Han, L. (2014). Highly compact TiO₂ layer for efficient hole-blocking in perovskite solar cells. *Applied Physics Express*, 7(5), 052301. <https://doi.org/10.7567/APEX.7.052301>
- Yang, T., Park, S., Kim, T. G., Shin, D. S., Suh, K., & Park, J. (2017). Ultraviolet photodetector using pn junction formed by transferrable hollow n-TiO₂ nano-spheres monolayer. *Optics Express*, 25(25), 30843. <https://doi.org/10.1364/oe.25.030843>
- Ye, T., Xing, J., Petrovi  , M., Chen, S., Chellappan, V., Subramanian, G. S., Sum, T. C., Liu, B., Xiong, Q. & Ramakrishna, S. (2017). Temperature effect of the compact TiO₂ layer in planar perovskite solar cells: An interfacial electrical, optical and carrier mobility study. *Solar Energy Materials and Solar Cells*, 163, 242–249. <https://doi.org/10.1016/j.solmat.2017.01.005>
- Yoo, Y., Seo, G., Park, H.J., Kim, J., Jang, J., Cho, W., Kim, J.H., Shin, J., Choi, J.S., Lee, D., Baek, S.-W., Lee, S., Kang, S.M., Kim, M., Sung, Y.-E., Bae, S., 2024. Low-temperature rapid UV sintering of sputtered TiO₂ for flexible perovskite solar modules. *J Mater A Mater* 12, 1562–1572. <https://doi.org/10.1039/D3TA05666J>
- Zhang, S., Lei, L., Yang, S., Li, X., Liu, Y., Gao, Q., Gao, X., Cao, Q. & Yu, Y. (2016). Influence of TiO₂ Blocking Layer Morphology on Planar

Heterojunction Perovskite Solar Cells. *Chemistry Letters*, 45(6), 592–594. <https://doi.org/10.1246/cl.160059>



© 2025. The Author(s). This article is an open access article distributed under the terms and conditions of the Creative Commons Attribution-ShareAlike 4.0 (CC BY-SA) International License (<http://creativecommons.org/licenses/by-sa/4.0/>)